Deep ROSAT-HRI observations of the NGC 1399/NGC 1404 region: morphology and structure of the X-ray halo

M. Paolillo[1], G. Fabbiano[2], G. Peres[1], D.-W. Kim[2]

25 June 2001

ABSTRACT

We present the analysis of a deep (167 ks) ROSAT HRI observation of the cD galaxy NGC 1399 in the Fornax cluster, comparing it with previous work on this galaxy and with recent *Chandra* data. We find, in agreement with previous observations, an extended and asymmetric gaseous halo with a luminosity (in the 0.1-2.4 keV energy band) of $L_X = (5.50 \pm 0.04) \times 10^{41}$ erg s^{-1} within 46 kpc (assuming a distance of D=19 Mpc). Using both HRI and, at larger radii, archival PSPC data, we find that the radial behavior of the X-ray surface brightness profile is not consistent with a simple Beta model and suggests instead three distinct components. We use a multi-component bidimensional model to study in detail these three components that we identify respectively with the cooling flow region, the galactic and the cluster halo. From these data we derive a binding mass distribution in agreement with that suggested by optical dynamical indicators, with an inner core dominated by luminous matter and an extended dark halo differently distributed on galactic and cluster scales. The HRI data and a preliminary analysis of *Chandra* public data, allow us to detect significant density fluctuations in the halo. We discuss possible non-equilibrium scenarios to explain the hot halo structure, including tidal interactions with neighboring galaxies, ram stripping from the intra-cluster medium and merging events.

In the innermost region of NGC 1399, the comparison between the X-ray and radio emission suggests that the radio emitting plasma is displacing and producing shocks in the hot X-ray emitting gas. We do not detect the nuclear source in X-rays and we pose an upper limit of $\sim 4 \times 10^{39}$ erg s^{-1} (0.1-2.4 keV) to its X-ray luminosity.

We found that the NGC 1404 halo is well represented by a single symmetric Beta model and follows the stellar light profile within the inner 8 kpc. The mass distribution is similar to the 'central' component of the NGC 1399 halo. At larger radii ram pressure stripping from the intra-cluster medium produces strong asymmetries in the gas distribution.

Finally we discuss the properties of the point source population finding evidence of correlation between the source excess and NGC 1399.

Subject headings: X-rays: individual (NGC 1399, NGC 1404)—galaxies: halos—galaxies: clusters: individual (Fornax)—galaxies: jets—radio continuum: galaxies

[1]Università di Palermo - DSFA - Sez.di Astronomia, P.zza del Parlamento 1, 90134 Palermo; paolillo@astropa.unipa.it, peres@astropa.unipa.it

[2]Harvard-Smithsonian Center for Astrophysics, High Energy Division, 60 Garden St., Cambridge, MA 02138; pepi@head-cfa.harvard.edu, kim@head-cfa.harvard.edu

1. INTRODUCTION

NGC 1399 is the central dominant galaxy of the Fornax cluster. Due to its proximity (19 Mpc for $H_0 = 75$ km s^{-1} Mpc^{-1}), this very regular, almost spherical (E0; Ferguson 1989) cD galaxy has been extensively studied in a wide range of wavelengths, ranging form radio to X-rays. The optical radial profile, first studied by Schombert (1986) and later

in more detail by Killeen & Bicknell (1988), reveals a large halo extending up to 250 kpc. The galaxy is surrounded by a large number of globular clusters, 10 times in excess with respect to those of its nearer companion NGC 1404 and of the Fornax galaxy NGC 1380 (Kissler-Patig et al. 1999). Dynamical studies of the stellar population of NGC 1399 indicate that the central regions of the galaxy are characterized by a high velocity dispersion, decreasing with radius, and slow rotation, as expected in giant ellipticals (Graham et al. 1998). At larger radii the velocity dispersion starts increasing again, as shown by studies of the planetary nebulae (Arnaboldi et al. 1994) and globular clusters dynamical properties (Grillmair et al. 1994). This suggests a different dynamical structure, than that of the inner stellar body, for the galaxy envelope and the globular cluster population.

NGC 1399 hosts a weak nuclear radio source (Killeen, Bicknell & Ekers 1988) with radio luminosity of $\sim 10^{39}$ ergs s^{-1} between 10^7 and 10^{10} Hz. The radio source has two jets ending in diffuse lobes, confined in projection within the optical galaxy. Killeen, Bicknell & Ekers (1988) suggest that the radio source is intrinsically small and confined by the thermal pressure of the hot ISM.

X-ray data have shown the presence of an extended hot gaseous halo surrounding NGC 1399. Observations made with the *Einstein* IPC by Kim, Fabbiano & Trinchieri (1992) constrained the gas temperature to be kT>1.1 keV. The *Einstein* IPC data were used also by Killeen & Bicknell (1988) to derive the mass distribution of the galaxy. They found that both models with and without dark matter were compatible with those data, depending on the assumed temperature profile. White (1992) suggested the presence of a cooling flow in the center of the galaxy, depositing 0.8±0.6 $M_\odot$ y^{-1}. Ginga observations (Ikebe et al. 1992) led to the detection of extended emission out to a galactocentric radius of ∼250 kpc. Serlemitsos et al. (1993) constrained the X-ray temperature to be 1.0<kT<1.5 keV with the Broad Band X-ray Telescope. **?**) hereafter RFFJ]rang95, using the Rosat PSPC, have studied in detail the temperature profile of the hot inter-stellar medium (ISM) out to 220 kpc finding an isothermal profile (0.9<kT<1.1) from 7 to 220 kpc, and a central cooling flow (0.6<kT<0.85) of at least 2 $M_\odot$ y^{-1}.

Ikebe et al. (1996) were able to identify with ASCA the presence of different components in the X-ray halo, associated respectively with the galaxy and the Fornax cluster potential. Jones et al. (1997) used the better resolution of the Rosat PSPC for studying in detail the cluster X-ray structure and finding a total binding mass of (4.3-8.1)×10^{12} $M_\odot$ within 100 kpc, with a mass-to-light ratio increasing from 33 $M_\odot/L_\odot$ at 14 kpc to 70 $M_\odot/L_\odot$ at 85 kpc. They also found a metal abundance of 0.6 solar.

Buote (1999) analized ASCA data finding that either a two temperature spectral model or a Cooling-Flow model with Fe solar abundances, are required to fit the thermal X-ray emission, and additional absorption is needed in the galaxy center. Matsushita, Ohashi & Makishima (2000) found similar near solar metallicities but argued that the metallicity inferred by ASCA spectral fits is dependent on the assumed atomic physics model and is not solved by muti-components spectral models.

More recently Sulkanen & Bregman (2001) used ROSAT data to pose an upper limit on the nuclear source brightness. The *Chandra* data were used by Loewenstein et al. (2001) to further constrain the nuclear source and by Angelini, Loewenstein & Mushotzky (2001) to study the point source population hosted by globular clusters.

In this paper we present the results of a deep image of the NGC 1399–NGC 1404 field obtained from data collected between 1993 and 1996 with the ROSAT High Resolution Imager (HRI, for a description see Dav96). We take advantage of the $\sim$ 5" resolution of the HRI to study in detail the structure of the galactic halo and relate the results to those obtained at larger scales with poorer resolution instruments. We study the interactions between the nuclear radio source and the galactic halo and discuss the properties of the discrete sources population. A preliminary analysis of *Chandra* data supports the Rosat results. Throughout this paper we adopt $H_0 = 75$ km s^{-1} Mpc^{-1} and a distance of 19 Mpc (1'=5.5 kpc).

2. OBSERVATIONS AND DATA ANALYSIS

The NGC 1399 field, including NGC 1404, was observed at three separate times with the ROSAT HRI: in February 1993, between January

Table 1: Rosat HRI observations of NGC 1399.

name	Field center		sequence id.	Exp.time	obs. date	P.I.
	R.A.	Dec		(sec)		
NGC 1399	$03^h38^m31^s$	–35°27'00"	RH600256n00	7265	1993 Feb 17	D.-W. Kim
"	"	"	RH600831n00	72720	1996 Jan 04-1996 Feb 23	G. Fabbiano
"	"	"	RH600831a01	87582	1996 Jul 07-1996 Aug 26	G. Fabbiano

and February 1996 and between July and August of the same year. The total exposure time is 167.6 Ks (Table 1). The data were processed with the SASS7_8 and SASS7_9 versions of the ROSAT standard analysis software (SASS). For our data analysis, we used the IRAF/XRAY and CIAO packages developed at the Smithsonian Astrophysical Observatory and at the *Chandra* X-ray Center (CXC), and other specific software as mentioned in the text.

2.1. Aspect Correction

The HRI data processed with the SASS versions prior to SASS7_B of March 1999 (as it happens for our data) suffer from an error in the aspect time behavior (Harris 1999). This translates into an error on the position of the incoming photons and thus it results in a degradation of the Point Response Function (PRF). Because high resolution analysis is the primary objective of this work we run the correction routine ASPTIME (F. Primini 2000, private communication) on the data, to improve the aspect solution. Visual inspection of the brightest pointlike sources in our field (Figure 1) demonstrates the improvement in the image quality.

Additional problems that may preclude the attainment of the HRI potential resolution are the imperfect correction of the spacecraft wobble and the wrong tracking of reference stars due to the variable pixel sensitivity across the detector (Harris et al. 1998). We followed the procedure suggested by Harris and collaborators, of dividing the observations in time bins (OBI) and realigning these segments by using the centroids of a reference pointlike source in each OBI.

Our data can be divided in 4 OBIs in RH600256n00, 43 in RH600831n00 and 33 in RH600831a01. We checked each OBI individually using the brightest point source in the field (No.8 in Table 3). We found that in the first observation (RH600256n00) the OBI are well aligned and no correction is needed. The second observation (RH600831n00) has 7 OBIs out of 43 that are 7"-10" displaced; however, the overall PRF is 6" FWHM so that just a slight improvement can be obtained dewobbling the image. The third observation (RH600831a01) has a 8" PRF but the signal to noise ratio of the individual OBIs is worse than in the previous observations so that the dewobbling procedure cannot be applied. Given these results, we decided not to apply the dewobbling correction, and to take as good a resulting PRF, in the composite image, of $\simeq$7" FWHM.

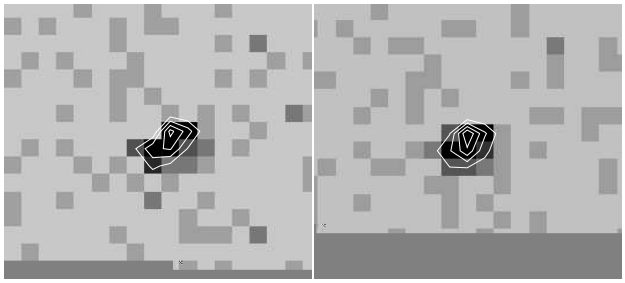

Fig. 1.— Comparison between the aspect of the brightest pointlike source in the NGC 1399/1404 field (No.8 in Table 3) before (left) and after (right) correction. The pixel size is 4". Contour levels are spaced by 5.9×10^{-2} cnts arcmin^{-2} s^{-1} with the lower one at 6×10^{-2} cnts arcmin^{-2} s^{-1}.

2.2. Composite Observation and Exposure Corrections

The aspect-corrected observations were coadded to obtain a "composite observation". To make sure that pointing uncertainties did not degrade the image we used the centroids of three bright pointlike sources in the field (No.8, 19 an 24 in Table 3) to align the images. The applied corrections were all within 2 arcsec. The resulting composite image is shown in Figure 2. This image

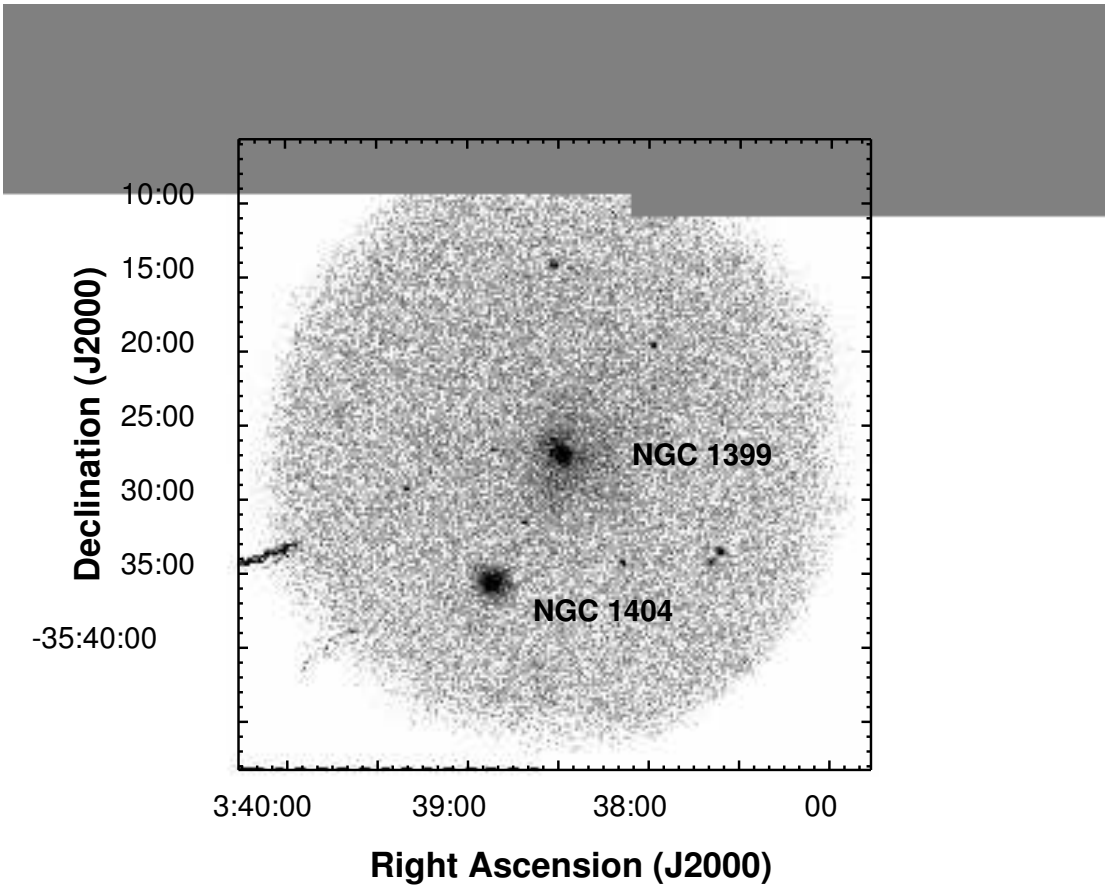

Fig. 2.— The 'raw' NGC 1399/NGC 1404 HRI field. The composite image is here displayed after it was rebinned to 5 arcsec/pixel. Even without exposure correction the extended emission surrounding NGC 1399 is clearly visible. The elongated features in the lower left corner are due to the presence of "hot spots" on the detector.

was then corrected for vignetting and variations of exposure time and quantum efficiency across the detector by producing an "exposure map" for each observation with the software developed by S.L. Snowden (Snowden et al. 1994, hereafter SMB).

2.3. Brightness Distribution and X-ray/Optical Comparison

To study the large-scale brightness distribution of the NGC 1399 field we rebinned the exposure corrected data in 5"×5" pixels. We then adaptively smoothed the image with the CXC CIAO *csmooth* algorithm which convolves the data with a gaussian of variable width (depending on the local signal to noise range of the image) so to enhance both small and large scale structures.

The resulting image (Figure 3a) shows a complex X-ray morphology. The center of the image is occupied by the extended halo of NGC 1399. The galaxy possess a central emission peak and an external extended and asymmetric halo. This halo is not azymuthally symmetric with respect to the X-ray peak, but it extends more on the SW side. The X-ray surface brightness distribution of the halo appears filamentary, with elongated structures and voids. As it can be seen from a comparison with the optical Digitized Sky Survey (DSS) image (Figure 3b), while the X-ray emission peak is centered on the optical galaxy, the X-ray halo extends radially much further than the optical distribution. Moreover most of the features seen in the X-ray image have no direct optical counterpart.

The X-ray emission of NGC 1404 instead is almost symmetric and largely consistent with the optical distribution, with the exception of the SE

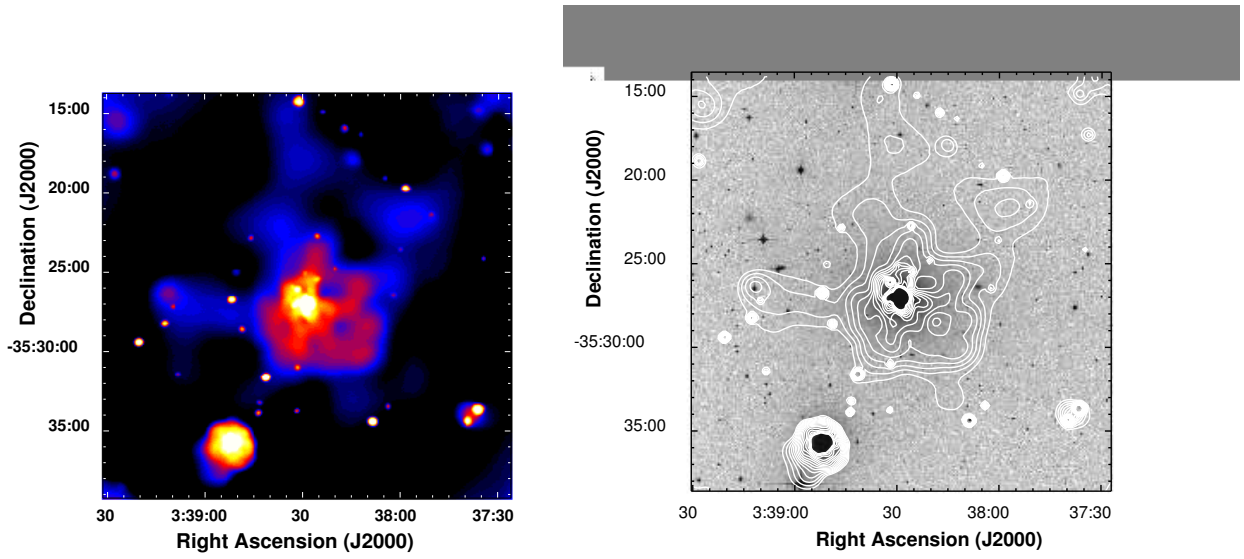

(a) (b)

Fig. 3.— (a) 5×5 arcsec/pixel adaptively smoothed image of the central part of the NGC 1399/1404 HRI field. Colors from black to yellow represent logarithmic X-ray intensities from 5.6×10^{-3} to 3.58×10^{-1} cnts arcmin^{-2} s^{-1}.(b) X-ray brightness contours overlaid on the 1 arcsec/pixel DSS image (logarithmic grayscale). Contours are spaced by a factor 1.1 with the lowest one at 6.1×10^{-3} cnts arcmin^{-2} s^{-1}. The X-ray emission peak is centered on the optical galaxy for both NGC 1399 and NGC 1404. In the case of NGC 1404 the X-ray isophotes are consistent with the optical distribution while in NGC 1399 the X-ray emission extends further out than the optical one.

tail reported by Jones et al. (1997) in the PSPC data, that may be the signature of ram pressure stripping of the NGC 1404 corona infalling toward the denser NGC 1399 cluster halo.

A number of pointlike source in the field is also evident in Figure 3a. The analysis of these sources is discussed in § 2.9.

We examined the inner halo of NGC 1399 in greater detail using a 1"/pixel resolution. The adaptively smoothed image (Figure 4) reveals an elongation of the inner halo structure in the N-S direction plus a large arc protruding to the West side of the halo. Several voids are present in the X-ray distribution, the largest being 1.5 arcmin NW of the emission peak. The central peak appears circular with at most a slight N-S elongation.

These features are all above 3σ significance, since 3σ was the minimum significance level requested for an intensity fluctuations to be smoothed on a given scale. Some features, as the SW clump centered at RA, Dec=$3^{\rm h}38^{\rm m}15^{\rm s}$,–35°29'00" or the one at $3^{\rm h}39^{\rm m}10^{\rm s}$,–35°26'30", are also detected with a wavelets detection algorithm (see § 2.9). We can rule out that features on scales of 1 arcmin are of statistical nature, because their significance can be as high as 6σ (see § 2.5). These brightness fluctuations must be due to the local physical conditions of the hot gaseous halo.

2.4. Radial Brightness Profiles

2.4.1. NGC 1399

As a first step in the quantitative study of the X-ray emission, we created a radial profile from the HRI data, assuming circular symmetry. Count rates from the exposure-corrected composite image, were extracted in circular annuli centered on the X-ray centroid RA, Dec=$3^{\rm h}38^{\rm m}28^{\rm s}.9$, –35°27"02'.1. We took care to remove the contribution of all the detected point-like sources by excluding circles within the 3σ radius measured by the wavelets algorithm (§ 2.9), from the source